Atmospheric Turbidity of Solar Radiation over Langtang National Park

Prakash M. Shrestha, Indra B. Karki, Narayan Prasad Chapagain and Khem N. Poudyal

Journal of Nepal Physical Society
Volume 8, No 1, 2022
(Special Issue: ICFP 2022)
ISSN: 2392-473X (Print), 2738-9537 (Online)

JNPS, **8** (1), 63-69 (2022)
DOI: http://doi.org/10.3126/jnphyssoc.v8i1.48288

Published by: Nepal Physical Society
P.O. Box: 2934
Tri-Chandra Campus
Kathmandu, Nepal
Email: nps.editor@gmail.com

ICFP 2022
ISSN:2392-473X (Print)
2738-9537 (Online)

Research Article ©Nepal Physical Society
DOI:http://doi.org/10.3126/jnphyssoc.v8i1.48288

Atmospheric Turbidity of Solar Radiation over Langtang National Park

Prakash M. Shrestha,[1, a)] Indra B. Karki,[1] Narayan P. Chapagain,[2] and Khem N. Poudyal[3]

[1)]*Department of Physics, Patan Multiple Campus, IoST, TU*

[2)]*Department of Physics, Amrit Campus, IoST, TU*

[3)]*Department of Physics, Department of Physics, Pulchowk Engineering Campus, IoE, TU*

[a)]*Corresponding author: prakash.shrestha@pmc.tu.edu.np*

Abstract. *The main aim of this project is to study atmospheric turbidity of solar radiation over Langtang National Park (28.2112^o N, 85.5663^o E and altitude 3862 m a.s.l.). The daily aerosol optical depth (AOD) data are derived from Aerosol robotic network (AERONET) for a period of one year 2018. Annual mean of Angstrom exponential(α), Angstrom turbidity coefficient (β) and curvature of AOD (a_2) are found 1.04 $\pm$ 0.29, 0.03$\pm$ 0.02 and 4.1 $\pm$ 0.9 respectively. The average value of and Linke turbidity (L_T) is 2.5 $\pm$ 0.6. Result of this research work is beneficial for the further identification, impact and analysis of atmospheric turbidity factors at different places.*

Keywords:
Aerosol optical depth, Angstrom turbidity coefficient, Angstrom exponential, curvature of AOD, Linke turbidity.

Received: 23 March 2022;**Revised**: 20 April 2022; **Accepted**: 12 May 2022

INTRODUCTION

Sun radiates 4×10^{26} J energy per second. Out of that energy, 1367 W/m^2 (solar constant) incidents on outer layer of atmosphere when Earth is at distance 1.49×10^8 km from The Sun [1]. The Solar radiation interacts with large particle of atmosphere such as water droplets, dust and aerosol. According to Beer Lambert's law, the solar radiation decreases exponentially with extinction coefficient (k) and optical air mass (m) in atmosphere [2]. The extinction of solar radiation is sum of extinction due to gas mixture, water vapor, ozone, aerosol and Rayleigh scattering. Aerosols are suspension solid and liquid particle with size 1 nm to 10 μ m. Atmospheric aerosols are a minor constituent of the Earth's atmosphere, but they play an important role in the energy balance of the earth–atmosphere system [3]. Both natural and anthropogenic aerosols influence on the solar radiation on three ways: directly by affecting the scattering and absorption of solar radiation, indirectly by altering cloud micro physics and lifetime and semi-directly by affecting cloud formation or evaporation [4, 5]. One of anthropogenic aerosols, black carbon are emitted by vehicles and kilns, produces green house effect. It melts ice on mountain. Vehicle also emits particular matter (such as PM10, PM2.5), are responsible for respiratory illness. The opacity of atmosphere for the solar energy gives atmospheric turbidity.The measurement of atmospheric aerosol physical and optical properties can provide knowledge of understanding the role of aerosols in the climate system. There are large number of atmospheric turbidity index. Angstrom turbidity coefficient(β), Angstrom exponential (α) and Linke tubidity (L_T) are used mostly used [6]. The spectral variation of aerosol optical depth (AOD) gives a picture of aerosol size distribution. The variability of aerosol size distribution is a good indicator for the sources of aerosols.

Nepal is a south east mountainous Asian country with beautiful landscape. Within this area ,there are diversity in biosphere and variation of climate [7]. In developing countries like Nepal, the most of energy consumption is fuel wood, agriculture residue, cow dung, coal and petroleum product. There is only 2.1% [8] of clean energy hydro-power, is used through the country. It means that rest of energy is conventional energy. About 0.4 millions vehicle register in Nepal in 2018 [9]. So it emits large amount of carbon dioxide and other harmful gases such as nitrous oxide, methane, carbon mono oxide etc. Large foreign currency is used to export petroleum product. Due to petroleum fuel based vehicle, air pollution increases. Study of atmospheric turbidity and its dependence on different meteorological parameters are used agriculture, Hydrology, Climate change, energy harvesting. Angstrom exponent (α), Angstrom turbidity coefficient (β) in Kathmandu on 1999 are 0.6247 $\pm$ 0.023 and 0.2997 $\pm$ 0.009 respectively [10]. Linke turbidity is 1.97$\pm$ 0.47 on Jumla on 2012 [11]. Linke turbidity is 5.53$\pm$ 0.23 on Kathmandu Valley on 2012 [12]. Linke turbidity is 5.7 $\pm$ 2.5 on Bhaktpur on 2013 [13]. Average seasonal value of Angstrom exponential (α) are 1.14 $\pm$ 0.01 in winter, 1.17 $\pm$ 0.07 in the pre monsoon season, 1.10 $\pm$ 0.08 in monsoon and 1.22 $\pm$ 0.08 in the post monsoon season on Pokhara between 2010 and 2018 [14].

Langtang National Park (28.2112^o N, 85.5663^o E and altitude 3862 m a.s.l.) is Nepal's first Himalayan national park. It is the country's fourth-largest national park and spreads over 1.7 square km of land. The national park lies in the districts of Nuwakot, Sindhupalchowk and Rasuwa in the central Himalayan region of Nepal [15]. The conservation area is recorded to have over 70 glaciers of different sizes, the Ganesh Himal and Langtang mountain ranges.The place is known for lakes lying at very high altitudes like the Gosaikunda, Suryakunda, Dudhkunda, Bhairavkunda, and Parvatikunda. Gosaikunde lake is said to have been created by Shiva who struck the mountain with his Trishul to draw water so that he could his quench his thirst after drinking the Kalkut Bish (poison). Thousands of pilgrim goers from Nepal and India visit this place during Janai Purnima and Gangadashahara. The Langtang National Park is home to several high mountain peals like the Langtang Lirung, Langtang Ri, Dorje Lakpa, Changbu, Loenpo Gang, Yansa Tsenji [16]. The wildlife area experiences a wide variety of climatic zones ranging from subtropical to alpine.The Langtang Valley mostly experiences the southwest summer monsoon. The national park receives its annual rainfall between June and September. However, the days are warm and sunny during April, May, October, and November [17]. The grasslands of the area are natural grazing grounds for animals like Himalayan tahr and musk deer. Other animals like the Himalayan Black bear, red panda, wild dog, ghoral, snow leopard, and Assam macaque are also found in the wildlife reserve. The national park is also known to have recorded the flight of 250 different species of birds. Thai Airways, Airbus A310 carrying 113 people crashed into the park on 31 July 1992. The Langtang village was destroyed by an avalanche which was followed by the earthquake of April 2015. Map od Langtang National park is shown in figure 1.

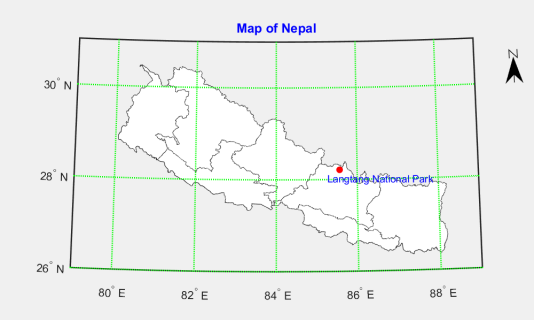

FIGURE 1: Map of Langtang National park[source:department of survey,2020]

MATERIALS AND METHOD

The opacity of atmosphere for solar energy gives atmospheric turbidity. There various type of atmospheric turbidity index. Angstrom turbidity is one of index. According to Angstrom relation [18], AOD is

$$AOD = \beta\lambda^{-\alpha} \tag{1}$$

Angstrom exponential (α)gives particle size distribution and Angstrom turbidity coefficient (β)measures the aerosol concentration and accounts for all scattering constituents other than Rayleigh. Values of $\alpha \leq 1$ indicate size distributions dominated by coarse mode aerosols (radii ≥ 0.5 μm) that are typically associated with dust and sea salt, and values of $\alpha \geq 2$ indicate size distributions dominated by fine mode aerosols (radii ≤ 0.5 μm) that are usually associated with urban pollution and biomass burning [19]. α and β are calculated by linear regression method.

Angstrom turbidity coefficient (β) measures the aerosol concentration and accounts for all scattering constituents other than Rayleigh.Angstrom exponential (α) is particle size distribution. α and β are calculated by linear regression method

$$log(AOD) = log(\beta) - \alpha log(\lambda) \tag{2}$$

In Angstrom's formula, the errors in α and β arises due to error in AOD and the choice of wavelength (λ). Then second order polynomial equation between $log(AOD)$ and

$log(\lambda)$ can be used to get precise information of aerosol size distribution [20].

$$log(AOD) = a_0 + a_1\ log(\lambda) + a_2\ log(\lambda)^2 \quad (3)$$

Here coefficients a_0, a_1 and a_2 are constant. a_2 gives curvature of AOD. It gives information about the domination of fine mode aerosols and coarse mode aerosols in the air. Another atmospheric turbidity is Linke turbidity(L_T). According to Dogniaux (1974) [21], Linke turbidity factor is

$$L_T = (\frac{85+\gamma}{39.5e^{-w}+47.4} + 0.1) + (16 + 0.22w)\beta \quad (4)$$

Here γ is solar height(90 - θ_z) and w is water contend in cm. Solar zenith angle (θ_z) is function of solar declination(δ), latitude (ϕ)of the place, solar hour angle (ω) and day number of year(n_d) [22]

$$\theta_z = \cos^{-1}(sin\delta\ \sin\phi + \cos\delta\ \cos\phi\ \cos\omega) \quad (5)$$

$$\delta = 23.45\sin(\frac{360}{365}(284+n_d)) \quad (6)$$

where optical air mass is

$$m_a = \frac{P}{101325}\frac{1}{(\cos\theta_z + 0.15(93.885-\theta_z)^{-1.253})} \quad (7)$$

P is atmospheric pressure at the place.
The daily spectral aerosol optical depth data of Langtang National Park for one year 2018 measured by CIMEL-318 sun photometer are available in the AERONET homepage of NASA. Spectral bands are 675, 500, 440, 380 and 340nm are used for calculation.
Open source software Python 3.7 software is used to analysis data and plot graph. Mean($\bar{x}$) standard deviation (σ), coefficient variance (CV), quartiles (Q1, Q2, Q3), skewness (sk) and kurtosis (ku) are used as statistical tool. Standard error (SE) is used as error bar in graph. Data are presented in form of mean $\pm$ standard deviation.

$$CV = \frac{\sigma}{\bar{x}} \times 100 \quad (8)$$

$$sk = \sqrt{\frac{\mu_3^2}{\mu_2^3}} \quad (9)$$

$$ku = \frac{\mu_4}{\mu_2^2} - 3 \quad (10)$$

where mu_4, mu_3 and mu_2 are fourth, third and second moments about mean.

RESULTS AND DISCUSSION

Figure 2(a) indicates daily variation of Angstrom exponential(α). The Maximum value of α is 2.34 in 167 of day number of year(DOY). Atmosphere contains fine mode aerosols. The minimum value of α is 0.15 in 158 of DOY. Atmosphere contains coarse mode aerosols. The annual average of α is 1.04 $\pm$ 0.29. The coefficient of variance(CV) is 26%. Figure 2(b) shows daily variation of Angstrom turbidity coefficient (β). The Maximum value of β is 0.284 in 86 of DOY. The minimum value of β is 0.001 in 167 of DOY. The annual average of β is 0.030 $\pm$ 0.029. The coefficient of variance is 97%. β varies large. Figure 2(c) shows daily variation of curvature of AOD (a_2). The Maximum value of a_2 is 8.4 in 167 of DOY. The minimum value of a_2 is 1.1 in 87 of DOY. The annual average of a_2 is 4.1 $\pm$ 0.9. The coefficient of variance is 21%. Figure 2(d) shows daily variation of Linke turbidity(L_T). The Maximum value of L_T is 6.9 in 86 of DOY. The minimum value of L_T is 1.8 in 226 of DOY. The annual average of L_T is 2.5 $\pm$ 0.6. The coefficient of variance is 25%. Statistics of those parameters are shown in Table 1.

TABLE I: Statistics of parameters

Parameters	α	β	a_2	L_T
Maximum	2.34	0.284	8.4	6.8
Minimum	0.15	0.001	1.2	1.8
Mean	1.04	0.030	4.1	2.5
sd	0.29	0.029	0.9	0.6
Q1	0.92	0.013	3.5	2.1
Q2	1.08	0.021	4.0	2.3
Q3	1.22	0.036	4.5	2.8
sk	-0.3	3.6	0.5	2.0
ku	2.3	21.7	2.3	7.9

Histogram of Angstrom exponential(α) is shown in figure 2(a). The first quartile (Q1), median (Q2) and third quartile(Q3) of α are 0.92, 1.08 and 1.22 respectively. The skewness of α (sk) is -0.3. The kurtosis of α (ku) is 2.3. The distribution is negative tailed and leptokurtic. L_T lies between 1.0 to 1.5 in 168 days. Histogram of Angstrom turbidity coefficient (β) is shown in Figure 2(b). The first quartile, median and third quartile of β are 0.013, 0.021 and 0.036 respectively.The skewness of β is 3. The kurtosis of β is 21.7. The distribution is positive tailed and leptokurtic. β lies between 0.2 to 0.3 in 243 days. Histogram of curvature of AOD (a_2) is shown in Figure 2(c). The first quartile, median and third quartile of a_2 are 3.5, 4.0 and 4.5 respectively. The skewness of a_2 is 0.5. The kurtosis of a_2(ku) is 2.3. The distribution is positive tailed and leptokurtic. a_2 lies between 3.0 to 4.0 in 112 days. Histogram of Linke turbidity(L_T) is shown in Figure 2(d). The first quartile, median and third quartile of L_T are 2.1, 2.3 and 2.8 respectively. The skewness

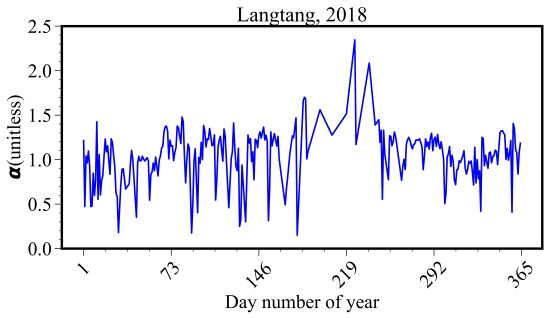

(a) Angstrom exponential

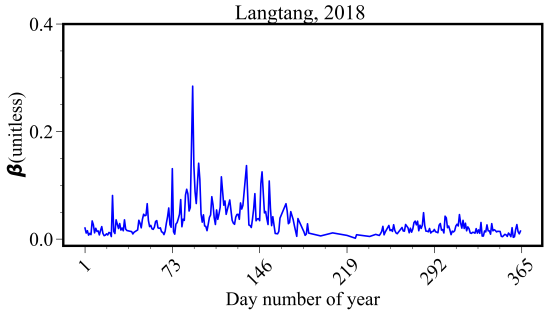

(b) Angstrom turbidity coefficient

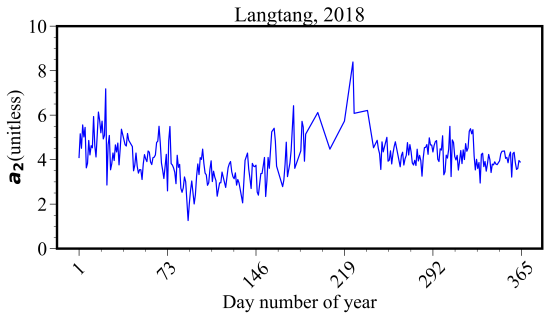

(c) Curvature of AOD

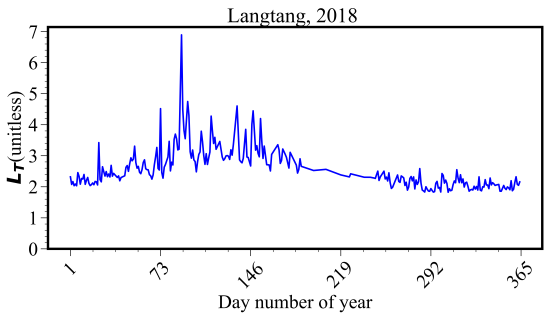

(d) Linke turbidity

FIGURE 2: Daily Variation of parameters

of L_T is 2.0. The kurtosis of L_T (ku) is 7.9. The distribution is positive tailed and leptokurtic. L_T lies between 2.0 to 3.0 in 186 days. Figure 4(a) indicates monthly variation of Angstrom exponential (α). The greatest value of α is 1.70± 0.44 in August due to rainy season and least value is 0.86±0.29 in January due to clear day. α varies large (CV = 36%) in June whereas least varies (CV = 15%) in October. Figure 3(b) indicates monthly variation of Angstrom turbidity coefficient (β). The Maximum value of β is 0.060± 0.033 in April and minimum value of 0.012±0.006 in July. β varies large (CV = 108%) in March whereas varies least (CV = 35%) in September. Figure 3(c) indicates monthly variation of curvature of AOD(a_2). The Maximum value of a_2 is 6.2± 1.2 in August and minimum value of 3.2±0.6 in April. a_2 varies large (CV = 24%) in March whereas varies least (CV= 7%) in December. Monthly variation of Linke turbidity (L_T) is shown in Figure 4(d). The Maximum value of L_T is 3.3± 0.6 in April and minimum value of 2.0±0.1 in December. L_T varies large (CV = 29%) in March whereas varies least (CV = 2%) in August. Seasonal variation of Angstrom exponential (α) is indicated by figure 4(a). The Maximum value α is 1.2± 0.2 in summer and minimum value is 1.9±0.1 in winter.The Maximum value coefficient of variance α is 19% in summer and minimum is 10% in autumn. Seasonal variation of Angstrom turbidity coefficient (β) is indicated by Figure 4(b). The Maximum value of β is 0.053±0.040 in spring and minimum value of 0.018±0.011 in winter. The Maximum value coefficient of variance of β is 75% in spring and minimum is 44% in autumn. Seasonal variation of curvature of AOD (a_2) is shown in Figure 4(c). The Maximum value of a_2 is 4.5±0.9 in summer and minimum value of 3.4±0.7 in spring. The Maximum value coefficient of variance of a_2 is 21% in summer and minimum is 12% in autumn. Seasonal variation of Linke turbidity (L_T) is shown in Figure 4(d). The Maximum value of L_T is 3.2± 0.6 in spring and minimum value of 2.1±0.2 in Autumn. The Maximum value coefficient of variance of L_T is 21% in spring and minimum is 8% in autumn. Fourier series is used to analysis seasonal variation of parameters.

$$y_s = a_o + a_1 \cos(\frac{2\pi}{365}x) + b_1 \sin(\frac{2\pi}{365}x) \qquad (11)$$

Offset is a_0 and seasonal amplitude is $\sqrt{a_1^2 + b_1^2}$. Figure 6(a) shows Fourier analysis of α. a_0 and seasonal amplitude are 1.07 and 0.14 respectively. Figure 6(b) shows Fourier analysis of β). a_0 and seasonal amplitude are 0.031 and 0.019 respectively. Figure 6(c) shows Fourier analysis of a_2. a_0 and seasonal amplitude are 4.1 and 0.4 respectively. Figure 6(d) shows Fourier analysis of L_T. a_0 and seasonal amplitude are 2.6 and 0.6 respectively.

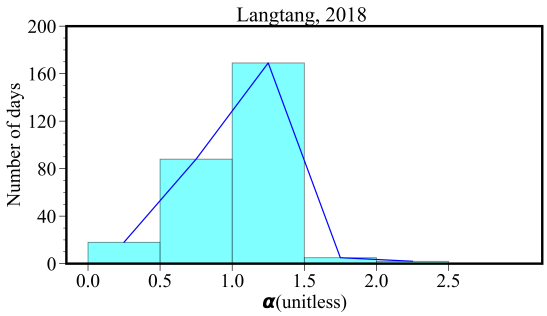

(a) Angstrom exponential

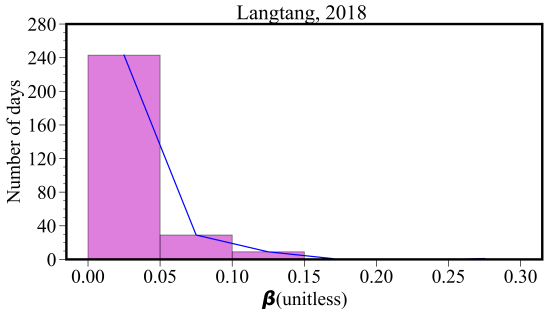

(b) Angstrom turbidity coefficient

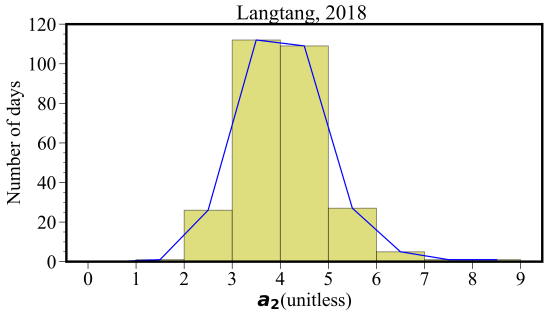

(c) curvature of AOD

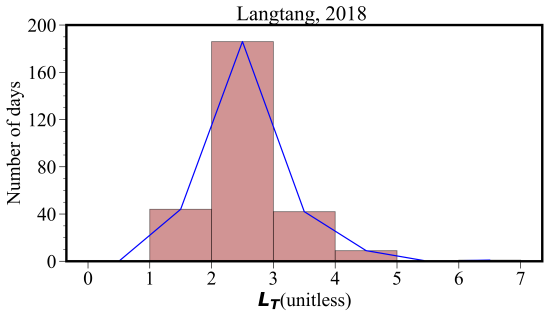

(d) Linke turbidity

FIGURE 3: Histogram of parameters

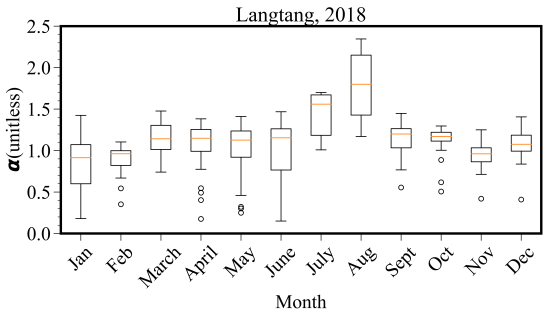

(a) Angstrom exponential

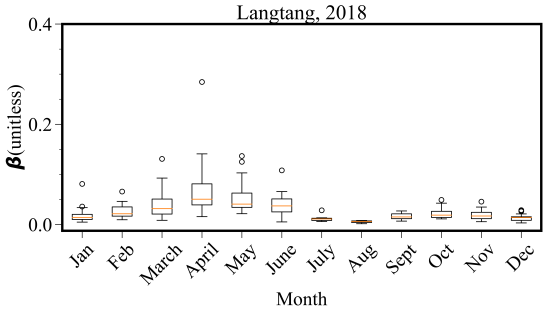

(b) Angstrom turbidity coefficient

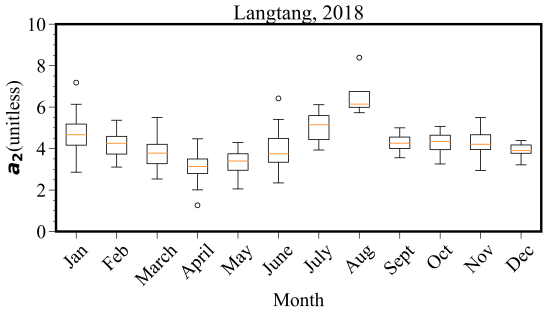

(c) curvature of AOD

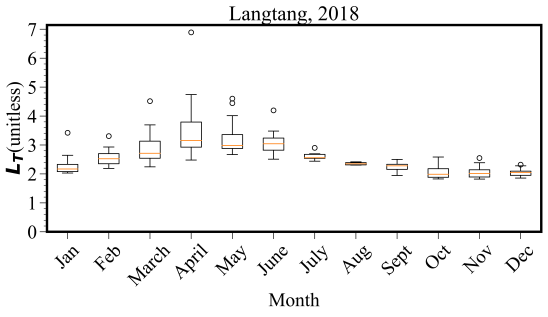

(d) Linke turbidity

FIGURE 4: Monthly Variation of parameters

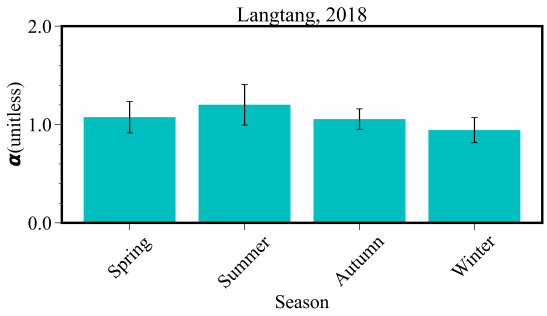

(a) Angstrom exponential

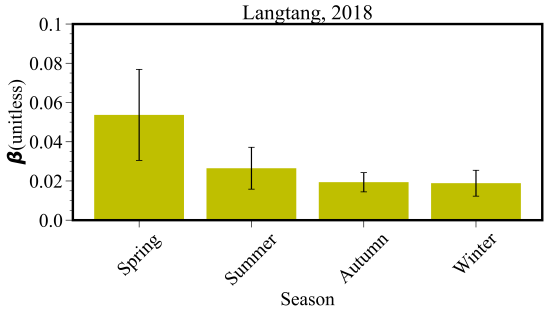

(b) Angstrom turbidity coefficient

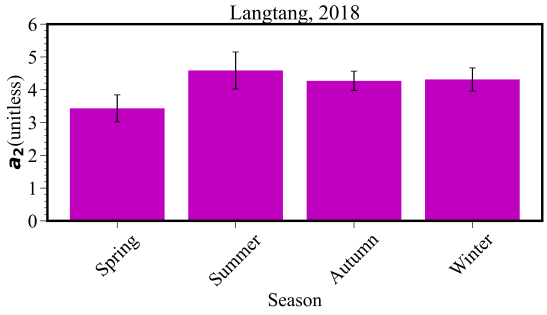

(c) Curvature of AOD

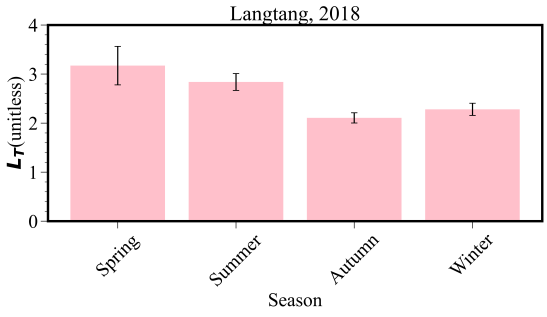

(d) Linke turbidity

FIGURE 5: Seasonal Variation of parameters

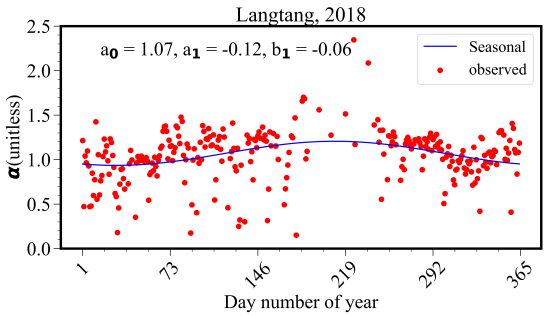

(a) Angstrom exponential

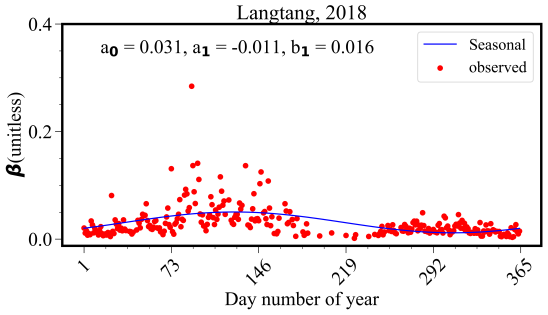

(b) Angstrom turbidity coefficient

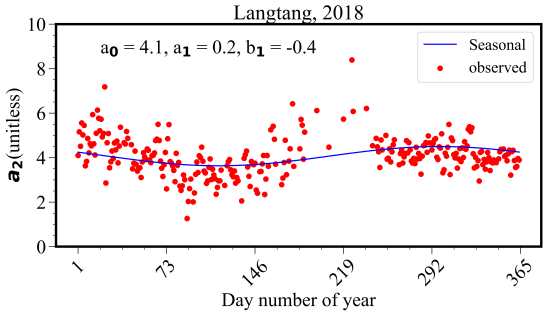

(c) Curvature of AOD

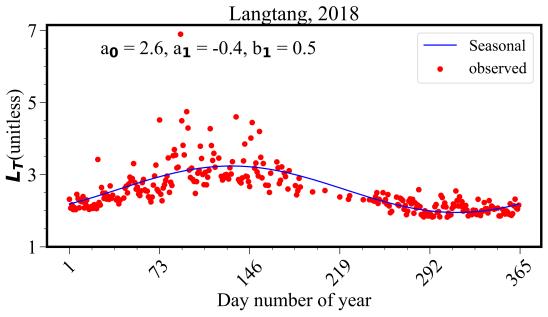

(d) Linke turbidity

FIGURE 6: Fourier analysis of parameters

CONCLUSIONS

The annual average of Angstrom exponential (α), Angstrom turbidity coefficient (β), curvature of AOD(a_2) and Linke turbidity (L_T) over the Langtang National Park are calculated for one year(2018) study period. α gradually increases from January to August.It varies large in June due to rain. Summer has large value. β increases from January to April and then decreases to July. Spring has large value. a_2 decreases from January to April and then increases to August. Summer has maximum value. L_T is maximum in April and then decreases to December. Spring has large value.

Linke turbidity is 3.3 to 7.7 in Wuhan ($30^0$32'N, $114^0$21'E, 30 m a.s.l.), Central China from 2010 to 2011 [23]. On eight years(1993 – 2000) study, Linke turbidity for four cities of India are 7.5 for Kolkata (26.93^0 N, 88.45^0 E, 431 m a.s.l.), 4.6 for Poona (18.53^0 N, 73.85^0 E, 559 m a.s.l.), 6.4 for Jaipur (26.93^0 N, 88.45^0 E, 431 m a.s.l.) and 6.8 for New Delhi(22.65^0 N,88.45^0 E, 216 m a.s.l.) [24]. From 2001 to 2004 at Qena (26.20^o N,32.75^o E, 96 m a.s.l.), Egypt, in hot season,T_L was 5.5 ± 0.26, in the cold seasons, T_L was 4.45 ± 0.44 [25]. A comparison of observed values of turbidity parameter with other major cities of the world shows that Langtang National Park is not polluted as cities like New Delhi, Qena, Kolkota, Jaipur etc.

ACKNOWLEDGMENT

The authors would like to convey our gratitude to faculty of CDP, Patan Multiple Campus, IoST for this opportunity as well as NASA for the data. We sincerely appreciate NAST for the PhD fellowship. We also like to acknowledge Nepal Physical Society(NPS) and Association of Nepali Physicists in America (ANPA) for educational workshop of Python.

REFERENCES

1. J. A. Duffie and W. A. Beckman, *Solar engineering of thermal processes* (John Wiley & Sons, 2013).
2. G. Lothian, "Beer's law and its use in analysis. a review," Analyst **88**, 678–685 (1963).
3. Y. A. Eltbaakh, M. H. Ruslan, M. Alghoul, M. Y. Othman, and K. Sopian, "Issues concerning atmospheric turbidity indices," Renewable and Sustainable Energy Reviews **16**, 6285–6294 (2012).
4. Y. J. Kaufman, D. Tanré, and O. Boucher, "A satellite view of aerosols in the climate system," Nature **419**, 215–223 (2002).
5. V. Ramanathan and G. Carmichael, "Global and regional climate changes due to black carbon," Nature geoscience **1**, 221–227 (2008).
6. M. Hussain, S. Khatun, and M. Rasul, "Determination of atmospheric turbidity in bangladesh," Renewable Energy **20**, 325–332 (2000).
7. M. R. K. Majupuria T C, *Nepal nature's paradise: insight into diverse facets of topography, flora and ecology* (M Devi,Gwalior,India, 1999).
8. MoF, *Economic Survey 2018/019* (Ministry of Finance, Government of Nepal, 2018).
9. DTM, *Register vehicles till fiscal year BS 2074/075* (Department of Transport Management,Ministry of physical infrastructure and transport,Government of Nepal, BS 2075).
10. B. Sapkota and R. Dhaubhadel, "Atmospheric turbidity over kathmandu valley," Atmospheric Environment **36**, 1249–1257 (2002).
11. P. M. Shrestha, I. B. Karki, N. P. Chapagain, and K. N. Poudyal, "Study of linke turbidity factor on solar radiation over jumla," Molung Educational Frontier **9**, 141–149 (2019).
12. P. M. Shrestha, K. N. Poudyal, N. P. Chapagain, and I. B. Karki, "Study of impact of linke turbidity on solar radiation over kathmandu valley," Patan Pragya **6**, 191–198 (2020).
13. P. Shrestha, N. Chapagain, I. Karki, and K. Poudyal, "Study of linke turbidity factor over bode, bhaktapur," Journal of Nepal Physical Society **6**, 66–73 (2020).
14. J. Regmi, K. N. Poudyal, A. Pokhrel, M. Gyawali, L. Tripathee, A. Panday, A. Barinelli, and R. Aryal, "Investigation of aerosol climatology and long-range transport of aerosols over pokhara, nepal," Atmosphere **11**, 874 (2020).
15. U. R. Bhuju, P. R. Shakya, B. T. Bd, and S. Shrestha, *Nepal Biodiversity Resource Book Protected Areas, Ramsar Sites, and World Heritage Sites* (ICIMOD ,UNEP, 2007).
16. P. N. Mishra, "The langtang national park:a proposed first biosphere reserve of nepal," Journal of National Science Foundation Sri lanka **31**, 333 – 335 (2003).
17. K. Sayers and M. A. Norconk, "Thimalayan semnopithecus entellus at langtang national park, nepal: Diet, activity patterns, and resources," Int J Primatol **29**, 509 – 530 (2008).
18. A. Angstrom, "Techniques of determinig the turbidity of the atmosphere," Tellus **13**, 214–223 (1961).
19. T. F. Eck, B. Holben, J. Reid, O. Dubovik, A. Smirnov, N. O'neill, I. Slutsker, and S. Kinne, "Wavelength dependence of the optical depth of biomass burning, urban, and desert dust aerosols," Journal of Geophysical Research: Atmospheres **104**, 31333–31349 (1999).
20. G. L. Schuster, O. Dubovik, and B. N. Holben, "Angstrom exponent and bimodal aerosol size distributions," Journal of Geophysical Research: Atmospheres **111** (2006).
21. R. Dogniaux, *Representations analytiques des composantes du rayonnement lumineux solaire: conditions de ciel serein* (Institut royal meteorologique de Belgique, 1974).
22. M. Iqbal, *An introduction to solar radiation* (New York: Academic Press, 1983).
23. L. Wang, Y. Chen, Y. Niu, G. A. Salazar, and W. Gong, "Analysis of atmospheric turbidity in clear skies at wuhan, central china," Journal of Earth Science **28**, 729–738 (2017).
24. L. Narain and S. Garg, "Estimation of linke turbidity factors for different regions of india," International Journal of Environment and Waste Management **12**, 52–64 (2013).
25. M. E.-N. Adam and E. F. El-Nobi, "Correlation between air temperature and atmospheric turbidity at a subtropical location," World Environment **7**, 1–9 (2017).